The G2019S LRRK2 Mutation Increases Myeloid Cell Chemotactic Responses and Enhances LRRK2 Binding to Actin-Regulatory Proteins

Mark S Moehle[1], João Paulo Lima Daher[1], Travis D Hull[2], Ravindra Boddu[3], Hisham A Abdelmotilib[1],James Mobley[2], George T Kannarkat[4], Malú G Tansey[4], and Andrew B West[1*]

[1] Department of Neurology and Center for Neurodegeneration and Experimental Therapeutics, [2]Department of Surgery, and [3]Department of Medicine, The University of Alabama at Birmingham, Birmingham, AL, 35294, USA
[4] Department of Physiology, Emory University School of Medicine, Atlanta, GA, 30322, USA.

*Corresponding Author:
Andrew B. West, Ph.D.
University of Alabama at Birmingham, CIRC Rm. 510, 1719 6th Ave. S.
Birmingham, AL 35294; Office Phone: (205) 996 7697
Fax: (205) 996 6580; Email: abwest@uab.edu

Supplemental Figure Legends

Figure S1. LRRK2 expression and baseline immune markers in non-transgenic and G2019S-LRRK2 rats. A) Representative western blot from primary macrophages derived from WT (non-transgenic, nTg) or G2019S(GS)-LRRK2 hemizygous rats. **B)** Macrophage cells cultured from GS-LRRK2 rats have a ~3 fold increase in LRRK2 expression, with LRRK2 signal normalized to actin signal. Three independent western blots were averaged, and effort bars are S.E.M. * is $p<0.01$, two-tailed unpaired t test. **C)** Representative confocal images of the substantia nigra pars compacta (SNpc) of 10-12 week old WT and GS-LRRK2 rats. Ionized calcium-binding adapter molecule 1 (Iba1), cluster of differentiation protein 68 (CD68), and tyrosine hydroxylase (TH), show no differences in the SNpc between strains of animals. Under normal conditions, CD68 cells, as shown, were very rarely observed through the SNpc of either WT or GS-LRRK2 rat SNpc. Iba1 signal was weak compared to TH expression and no signs of microgliosis could be detected in GS-LRRK2 rats compared to WT rats. Scale bars for images are 100 µm and 10 µm for “Zoom” fields.

Figure S2. Normal TH cell counts in adult G2019S-LRRK2 rats. A) Representative bright-field images of coronal sections of the SNpc from 10-12 week old WT non-transgenic (n=8) and G2019S-LRRK2 (GS-LRRK2, n=10) rats injected with saline

(ipsilateral) and sacrificed two weeks later. Sections were stained for TH using DAB stain (brown). **B)** Unbiased stereological quantification of TH cells as a percentage of the contralateral side of the WT (nTg) group. No significant differences could be detected in TH cell number of WT versus GS-LRRK2 animals, or in numbers of TH cells of ipsilateral versus contralateral sides ($p>0.5$ calculated with two-tailed Student's t-test, bars represent group means and error bars are S.E.M).

Figure S3. LRRK2 does not alter cytokine or chemokine release in TEPMs. Thioglycollate-elicited peritoneal macrophages (TEPM) cells were cultured from adult male non-transgenic littermate controls (WT, nTg), WT-LRRK2 BAC and G2019S(GS)-LRRK2 BAC mice (at least 3 animals per strain per experiment were used). TEPMs were allowed to rest overnight after plating onto dishes, and then cells were stimulated with LPS (100 ng ml^{-1}) for 6 hours. **A-E)** Quantification of representative secreted cytokines and chemokines as measured by a 32-plex mouse inflammation bead-array panel. There were no differences observed between groups for any detected secreted factor (one-way ANOVA, $p>0.5$). All bars represent group mean derived from at least three animals per strain, and error bars represent S.E.M.

Figure S4. G2019S-LRRK2 does not alter phagocytosis in TEPMs. Thioglycollate-elicited peritoneal macrophages (TEPM) cells were cultured from adult male non-transgenic littermate controls (WT, nTg), WT-LRRK2 BAC and G2019S(GS)-LRRK2 BAC mice (at least 3 animals per strain per experiment were used). **A)** TEPMs were allowed to rest overnight after plating and Zymosan beads were added to cultures at a ratio of 10:1 (bead per cell). The fluorescence of beads not internalized by the macrophages was eliminated with application of Sudan Black B reagent prior to imaging. The numbers of beads internalized per TEPM were determined from micrographs of live cells and histogram of beads phagocytized per TEPM of WT (nTg), WT-LRRK2, and GS-LRRK2 are shown. A reviewer blinded to genotype of the TEPMs counted the number of beads per cell. **B)** Representative images of TEMPs (phase-contrast) over-laid with labeled Zymosan beads (green fluorescence).

Figure S5. Flow cytometry gating strategy for TIP. Thioglycollate-induced peritoneal (TIP) cells obtained directly from lavage were first gated on forward/side scatter. Cells were then separated by CD11b and Ly6G(A18) intensities. Two populations emerged from this, CD11b+Ly6G(A18)- and CD11b+Ly6G(A18)+. The CD11b+Ly6G(A18)- was further analyzed by F4/80 and MHCII intensity. A majority (>65%) of the CD11b+Ly6G(A18)- population appeared to be weakly F4/80 positive but did not sufficiently diverge from isotype control. This is consistent with expected results from TIP cells. Only a small population of TIP cells (~25%) was MHCII positive indicative of monocytes/macrophages. CD11b+Ly6G(A18)+ cells were further analyzed by F4/80

and MHCII. A majority of the CD11b+Ly6G(A18)+ (>90%) were negative for both F4/80 and MHCII, likely making these cells neutrophils.

Figure S6. G2019S-LRRK2 expression does not alter baseline white blood composition. White blood cells were derived from at least three male adult mice each of WT (non-transgenic, nTg), WT-LRRK2 BAC, and G2019S(GS)-LRRK2. Red blood cells were lysed in each preparation and the remaining cells analyzed. **A)** Quantification of total white blood cells obtained by lavage of the unstimulated peritoneal cavity. **B,C)** Quantification of percentages of sub-classified white-blood cells from total cell population using flow cytometry. **D)** Representative histogram of MHCII fluorescent intensity of CD11b+Ly6G(A18)- cells from WT (nTg), WT-LRRK2, and G2019S(GS)-LRRK2 mice after TIP. **E)** Quantification of median fluorescent intensity (MFI) from panel D. No significant differences ($p>0.5$, One Way ANOVA) are observed between strains for all markers.

Figure S7. Gating strategy for CCR2 and CCR5. Thioglycollate-induced peritoneal (TIP) cells obtained directly from lavage were first gated on forward/side scatter. Cells were then gated on live cells by selecting for 7AAD- cells and separated by CD11b and Ly6G(A18) signal. The CD11b+Ly6G(A18)- and CD11b+Ly6G(A18)+ were then each analyzed by fluorescent intensity of CCR2 or CCR5.

Supplemental Figure 1.

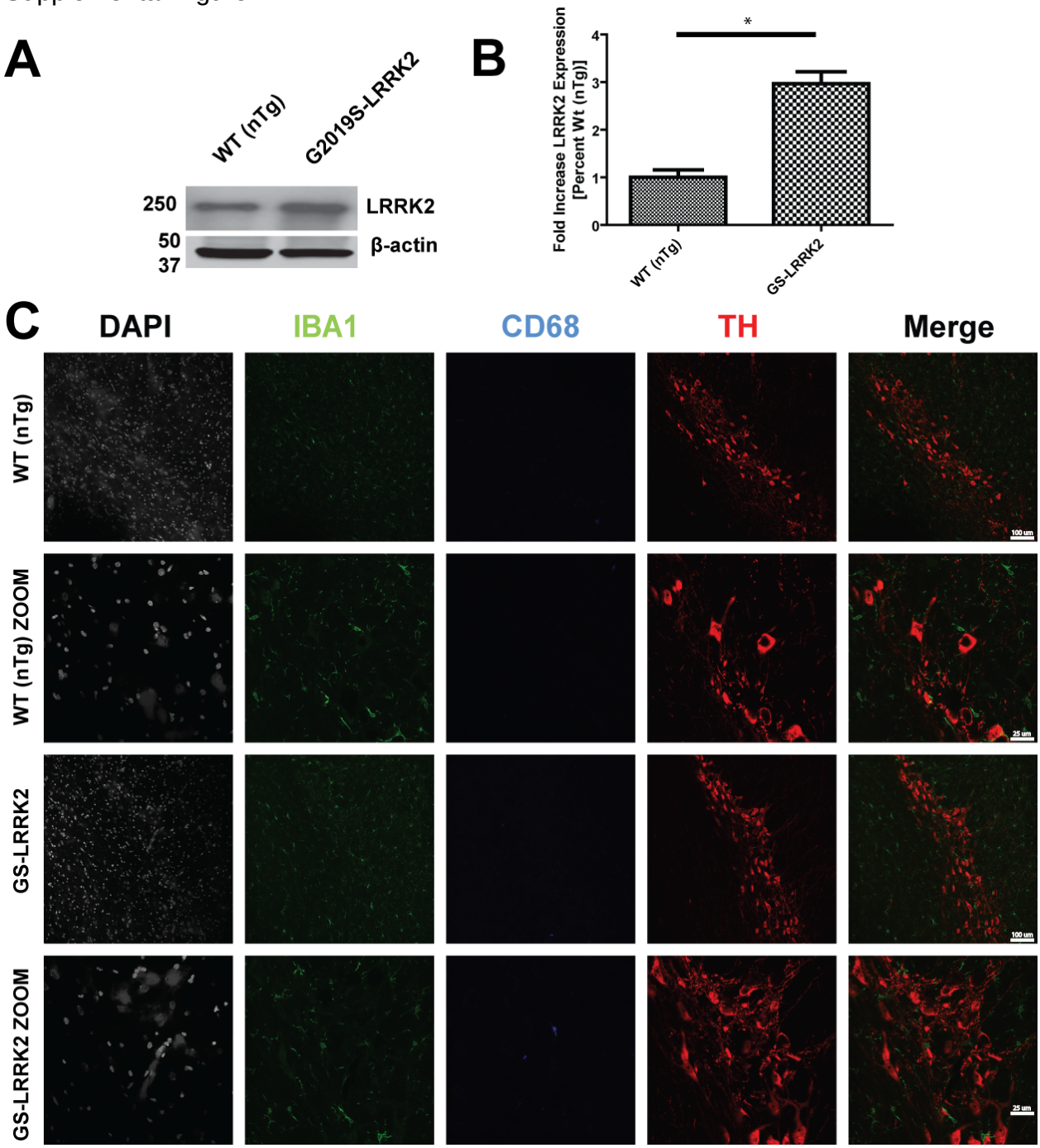

Supplemental Figure 2.

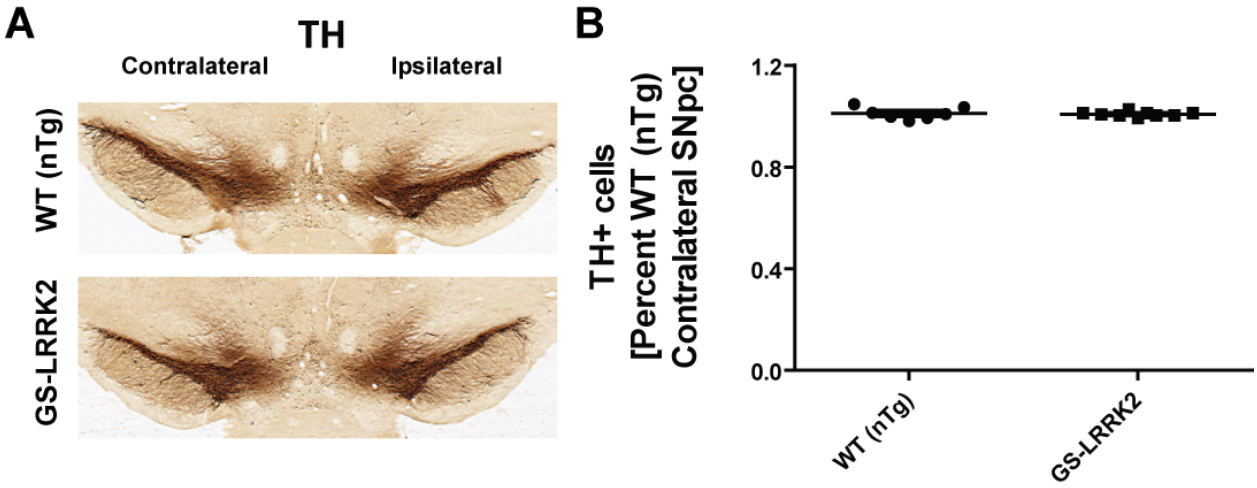

Supplemental Figure 3

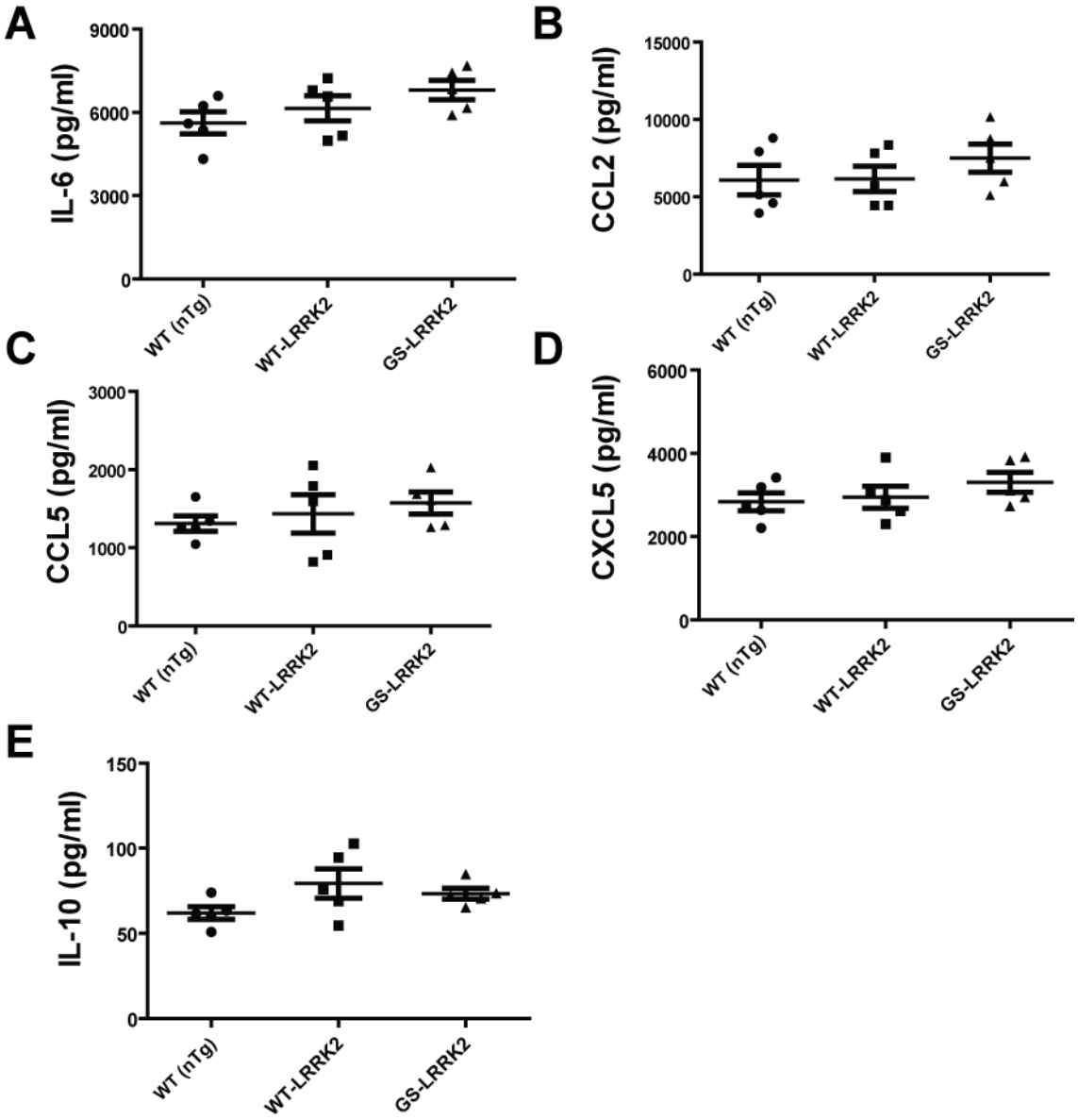

Supplemental Figure 4

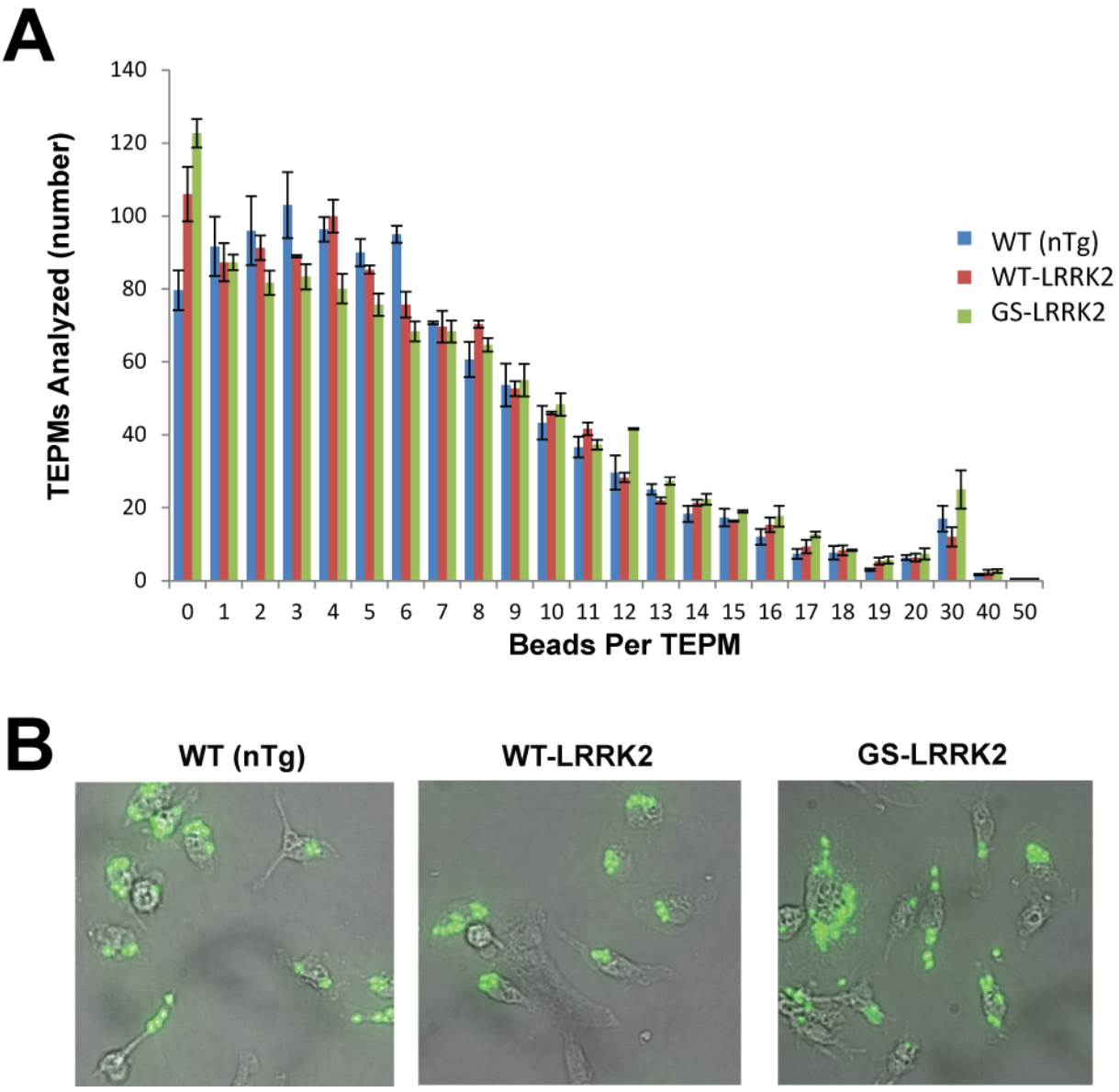

Supplemental Figure 5

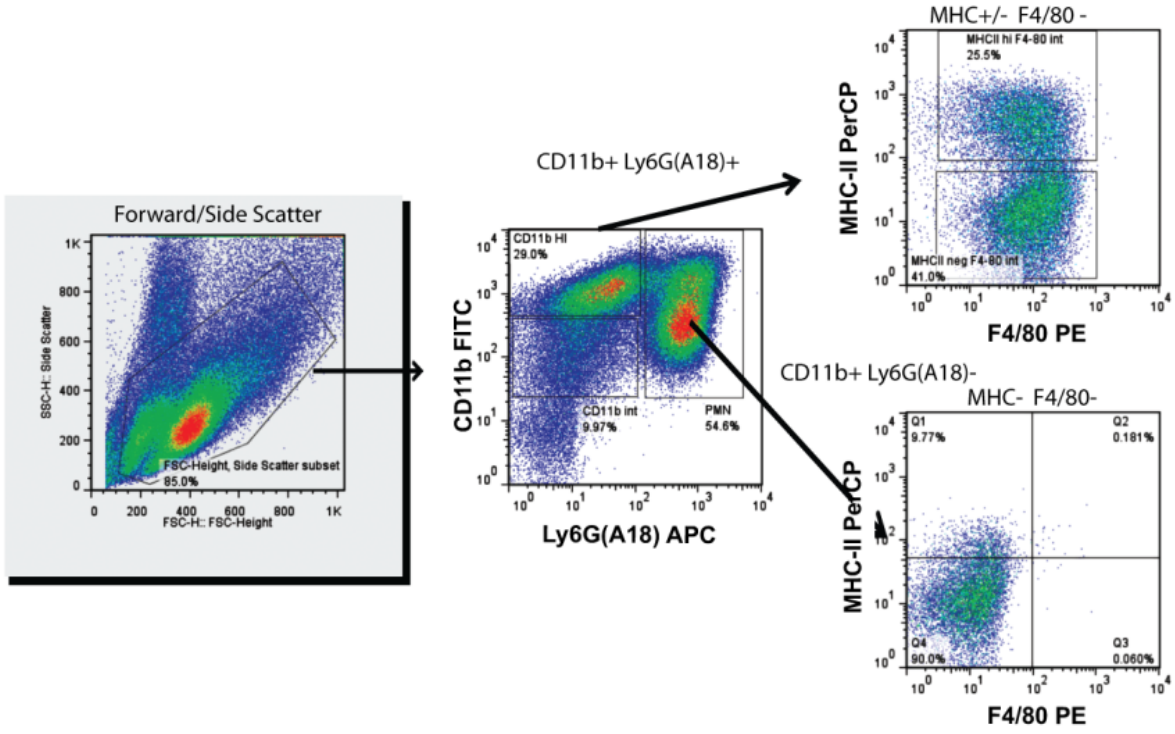

Supplemental Figure 6

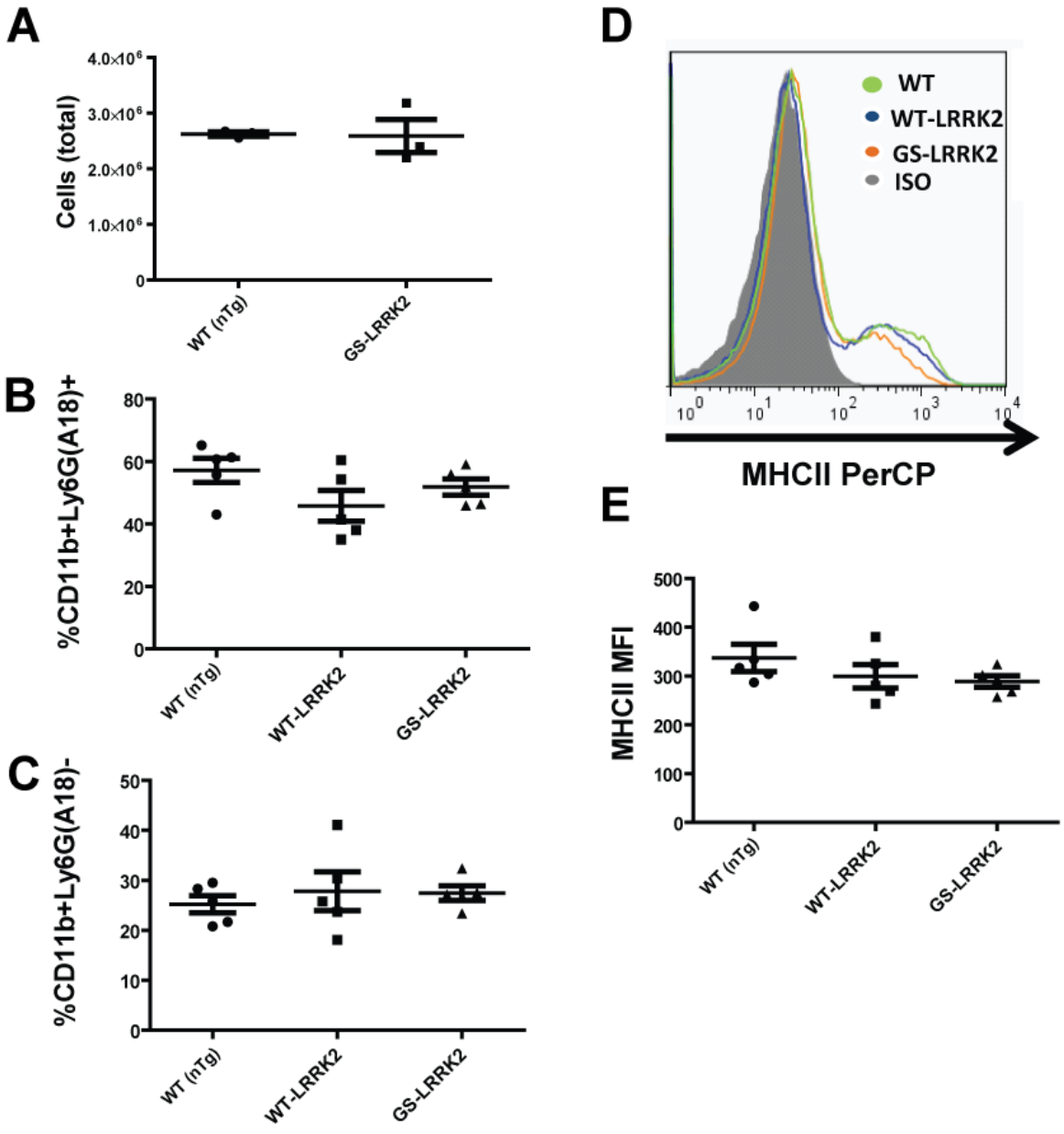

Supplemental Figure 7